A novel and simplified model of radiant fields in strongly forward scattering media: Shadow area model

Emine Kayahan[1], Senne Fransen[2], Leen Braeken[1], Tom Van Gerven[2], M. Enis Leblebici[1]

[1] *Center for Industrial Process Technology, Department of Chemical Engineering, KU Leuven, Agoralaan Building B, 3590 Diepenbeek, Belgium*

[2] Process Engineering for Sustainable Systems, *Department of Chemical Engineering, KU Leuven, Celestijnenlaan 200F, 3001 Leuven, Belgium*

*Corresponding author (muminenis.leblebici@kuleuven.be)

Abstract

Computing radiative fields in scattering media can be quite challenging due to the integro-differential nature of the radiative transfer equation. Several simplifications to this equation are suggested such as Beer's law, two-flux model (TFM) or six-flux model (SFM). Assumptions and final equations can differ depending on the field. For example, aerosol optics is often studied in length scales relevant to atmospheric sciences to study air pollution or cloud formation. The assumptions and approach adopted in aerosol sciences is different than the approach adopted in the field of photochemistry. In this work, we investigate the solution of radiative fields in aerosol photoreactors where there is a strong forward scattering. We are applying the equations used to compute radiative transfer equation in photocatalytic reactors to aerosol photoreactors with some adjustments. In addition, we suggest a novel approach to the solution of radiative transfer equation based on the shadow areas of the droplets. We showed that intersection areas of randomly distributed disks could be predicted by Poisson distribution. Then, shadow area model (SAM) was developed by a photon balance. Probability of forward and back scattering from several droplet diameters ranging between 5 to 300 µm were found by a ray tracing model in COMSOL Multiphysics. SAM is able to predict absorption and transmission with a similar accuracy to TFM and SFM. However, equations developed for SAM are simpler than TFM or SFM. Therefore, SAM provides an easier grasp of the physical phenomena.

1. Introduction

Process intensification efforts towards green chemistries accelerates the research in photoreactions. Photoreactions are considered green since they are usually fast, selective and require less solvent. Still, they are not utilized much in industry due to the difficulties of their scale up [1,2]. One of the strategies to scale-up micro-structured photoreactors is to create micro- or meso-structures in large scale vessels. Translucent packed-bed reactors and aerosol reactors can be considered as examples of such kinds of reactors [1]. Another novel approach is to use aerosol reactors for scaling up of photoreactors. In an aerosol reactor, liquid is broken down by a nozzle into droplets each of which work as microreactors. Therefore, aerosol photoreactors can be scaled up easily by increasing number of nozzles without compromising the microreactor reaction rates. As a result, aerosol photoreactors provide an exceptional platform for gas-liquid photoreactions. Due to the nature of the droplet-light interactions, light could be distributed well among the droplets. An aerosol photoreactor has been proven to increase conversions of several photooxygenation reactions significantly by a chemistry group [3–5]. Several singlet oxygen mediated oxidation reactions have been performed in aerosol photoreactors. Conversions larger than 90% were achieved for all the reactions in an aerosol reactor called NebPhotOX [6–8] in around one minute. In our previous work, almost full conversion were achieved under 16 s for a singlet oxygen mediated photosulfoxidation reaction. Furthermore, we showed that both light and mass transfer limitations can be overcome in an aerosol photoreactor even with a simple medical nebulizer [9]. Therefore, aerosol photoreactors were shown to work quite well. However, design of aerosol photoreactors still need to be optimized for an efficient scale-up.

Scale up of an aerosol photoreactor can be achieved by several strategies such as increasing concentrations of chemicals, aerosol volume concentration and/or number of nozzles. We showed that increasing concentration of a photosensitizer can lead to quenching of singlet oxygen, which limits the throughput [9]. Aerosol volume concentration is the total liquid volume in a unit volume. It can be increased by increasing droplet sizes and/or aerosol number concentration which is defined as number of droplets in a unit volume. Since volume of a droplet increases with the cube of its radius, aerosol volume concentration can be increased more easily by increasing droplet sizes. Here, it should be noted that increasing droplet sizes can lead to mass transfer limitations. In addition, aerosol number concentration and droplet sizes cannot be selected separately because they depend on the nozzle design. Up to now, a medical nebulizer [9] and a pneumatic nebulizer [6–8] were used in aerosol photoreactors. These nebulizers usually have low aerosol volume concentrations. For example, pneumatic nebulizers often require a gas to liquid volumetric ratio of a thousand. Ultrasonic nebulizers, on the other hand, can generate high aerosol volume concentrations [10]. In addition, they usually do not require a gas to atomize the liquid. Therefore, they might be better candidates for an efficient operation.

While scaling up aerosol photoreactors, mass and photon transfer limitations need to be considered. In our previous work, the convection-diffusion equation was solved by assuming that there was no convection. A simple equation was provided to check for critical droplet diameter where mass transfer limitations start [9]. Based on this solution, if characteristic reaction time is known, critical droplet diameter can be found easily. Therefore, while selecting a nozzle, droplet size distributions need to be considered to reduce or eliminate limitations arising from mass transfer. Apart from mass transfer considerations, an efficient operation depends on radiant field inside aerosol reactors. Radiant field inside an aerosol photoreactor depends on droplet sizes, aerosol number concentration, number of nozzles and diameter of the reactor (light path). However, which of these parameters makes the most difference in radiant field is not really known since radiant field in aerosol photoreactors has not been studied yet.

Solution of the radiative transfer equation is quite rigorous due to the integro-differential nature of the equation. Simplifications were proposed in several fields. Aerosol optics is studied in atmospheric sciences to predict cloud formation and air pollution. Therefore, the approach and assumptions used in aerosol sciences are not comparable to aerosol photoreactors. Radiant fields are computed in the field of photochemistry for photocatalytic applications. The models used in this field can be applied to aerosol photoreactors with slight changes.

In the field of photochemistry, Brucato and Rizzuti (1997) [11] proposed "zero reflectance model" (ZRM). This is the simplest model that can be used in slurry photoreactors. It assumes that when a photon hits a particle, it is completely absorbed. It also assumes that particles are not interacting with each other. This model is actually the same as Beer's law used for aerosols [10] except that Beer's law also accounts for particle extinction efficiency (Q_e) (Eq. (1)). In this model, reflected radiant flux is zero (Eq. (2)) whereas absorption is one minus transmitted radiant flux (Eq. (3)).

$$\boldsymbol{T_{BL}} = \frac{\boldsymbol{G_L}}{\boldsymbol{G_0}} = \boldsymbol{exp(-NA_pLQ_e)} \tag{1}$$

$$\boldsymbol{R_{BL}} = \boldsymbol{0} \tag{2}$$

$$\boldsymbol{A_{BL}} = \boldsymbol{1 - T_{BL} - R_{BL}} \tag{3}$$

where T_{BL} , R_{BL} and A_{BL} is transmission, reflection from the front window and absorption calculated by Beer's law , respectively. G_L is the radiant flux at light path *L (m)*, *N* is the aerosol number concentration (m^{-3}), A_p is the projected area of droplets or catalyst particles, Q_e is the efficiency factor.

Before moving on the other models, we need to introduce some definitions. Particle extinction efficiency (Q_e) is defined as radiant power scattered or absorbed by a particle divided by radiant power geometrically incident on a particle. Values of Q_e ranges from 0 to 5. It approaches 2 as the ratio of particle diameter to wavelength increases (Figure 1). This ratio of particle size to wavelength is defined as the size parameter (α) [10]. Extinction efficiency is the summation of scattering efficiency (Q_s) and absorption efficiency (Q_a). The ratio of scattering efficiency to extinction efficiency is called single-scattering albedo (*R*) as shown in Eq. (4). Scattering efficiency and single scattering albedo can be computed from Mie's theory.

$$R = \frac{Q_s}{Q_e} = \frac{Q_s}{Q_s + Q_a} \tag{4}$$

where *R* is single-scattering albedo, Q_s is scattering efficiency, Q_e is extinction efficiency and Q_a is absorption efficiency.

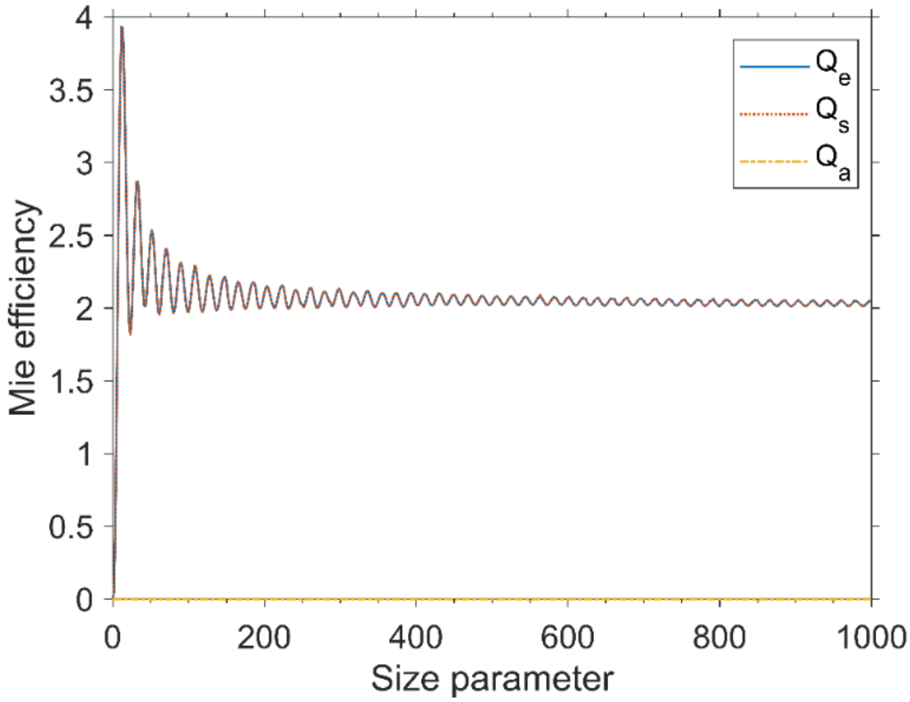

Figure 1. Extinction (Q_e), scattering (Q_s) and absorption (Q_a) efficiencies in terms of size parameter. Q_e and Q_s have approximately the same value, so cannot be differentiated in the graph and Q_a is zero. Refractive index of water at 600 nm was used during the calculations (n=1.33+1.39x10^{-8} i). Size parameter is defined as droplet size divided by wavelength. Calculations were based on Mie theory. MATLAB functions for the calculations were obtained from the report of Matzler [12].

In this paper, we will refer to ZRM as Beer's law. Beer's law overestimates absorption since it assumes all radiant flux is absorbed. However, in reality, some of the radiant flux is absorbed and some is scattered. Brucato et al. (1997) [13] proposed another simplification by using a two-flux model (TFM). TFM assumes that radiant flux moves in two directions: forward and backwards. It is commonly used to provide solutions for absorption or transmission in scattering media. The model that Brucato et al. [13] proposed assumes that when light hits a catalyst particle, it is either back-scattered or absorbed depending single-scattering albedo (R). Back-scattered light can be used by other catalyst particles. This model underestimates absorption since if light is allowed to move in other directions, there are more chances of a light ray to encounter other catalyst particles. Here, we call this model as TFM-1. The equations for TFM-1 are given in Eq. (5) to Eq. (9). Transmission is calculated by Eq. (5). Reflectance is calculated by Eq. (6). Absorption can be found by subtracting transmission and reflectance from one as shown in Eq. (7). Eq. (8) and Eq. (9) are used to calculate the terms in Eq. (5). This model is not expected to predict transmission or absorption through aerosols accurately since there is only back-scattering. However, aerosols with droplets in micron sizes or larger are expected to scatter most of the radiant flux in the visible region in the forward direction.

$$\boldsymbol{T_{TFM-1} = \frac{G_L}{G_0} = \left(\frac{1}{1-\eta}\right)\left(\exp\left(-\frac{x}{\lambda_R}\right) - \eta\exp\left(\frac{x}{\lambda_R}\right)\right)} \tag{5}$$

$$\boldsymbol{R_{TFM-1}} = \frac{\boldsymbol{g_0}}{\boldsymbol{G_0}} = \frac{\boldsymbol{1}}{\boldsymbol{R}}\left(\boldsymbol{1} - \frac{\boldsymbol{1+\eta}}{\boldsymbol{1-\eta}}\sqrt{\boldsymbol{1-R^2}}\right) \tag{6}$$

$$\boldsymbol{A_{TFM-1}} = \boldsymbol{1} - \boldsymbol{T_{TFM-1}} - \boldsymbol{R_{TFM-1}} \tag{7}$$

$$\eta = \frac{1-\sqrt{1-R^2}}{1+\sqrt{1-R^2}}\exp\left(-\frac{2L}{\lambda_R}\right) \tag{8}$$

$$\lambda_R = \frac{1}{NA_pQ_e\sqrt{1-R^2}} \tag{9}$$

where T_{TFM-1} is transmission calculated by TFM-1, G_0 is incoming radiant flux and G_L is forward radiant flux at length L, g_0 is the reflected radiant flux at position zero, x is any position, R is single scattering albedo, N is aerosol number concentration, A_p is projected area of one droplet, η is a dimensionless parameter, λ_R is extinction length and Q_e is extinction efficiency.

Following this work, Brucato et al (2006) suggested a six-flux model (SFM). In this model, light was allowed to follow six directions of the cartesian coordinates [14]. The SFM equations which was proposed by Brucato et al. [14] are given below (Eq. (10) - (18)). Transmission, reflectance and absorbance can be calculated by Eq. (10), Eq. (11) and Eq. (12), respectively. The rest of the equations (Eq. (13) – Eq. (18)) are used to calculate the terms in Eq. (10). A minor change was done to these equations. Brucato et al. [14] did not account for extinction efficiency in their calculations. In this work, extinction efficiency was added to Eq. (15). When the side scattering is assumed to be zero, the model simplifies to TFM with forward and back scattering (p_s=0). We call this as TFM-2 in this work. The parameters a (Eq. (16)) and b (Eq. (17)) are the only difference between TFM-2 and SFM. The model is simplified further to TFM-1 equations (Eq. (5) – Eq. (9)) when all radiant flux is assumed to be back-scattered (p_f=1, p_f=0 and p_s=0) [13]. Discretization of droplet diameters can be done by replacing the multiplication in Eq. (15) with Eq. (19) to account for the overall droplet size distribution.

$$\boldsymbol{T_{SFM}} = \frac{\boldsymbol{G_L}}{\boldsymbol{G_0}} = \left(\frac{\boldsymbol{1}}{\boldsymbol{1-\gamma}}\right)\left(\frac{\boldsymbol{2\sqrt{1-R_{corr}^2}}}{\boldsymbol{1+\sqrt{1+R_{corr}^2}}}\right)\mathbf{exp}\left(-\frac{\boldsymbol{L}}{\boldsymbol{\lambda_{R,corr}}}\right) \tag{10}$$

$$\boldsymbol{R_{SFM}} = \frac{\boldsymbol{g_0}}{\boldsymbol{G_0}} = \left(\frac{\boldsymbol{1}}{\boldsymbol{R_{corr}}}\right)\left(\boldsymbol{1} - \frac{\boldsymbol{1+\gamma}}{\boldsymbol{1-\gamma}}\right)\sqrt{\boldsymbol{1-R_{corr}^2}} \tag{11}$$

$$\boldsymbol{A_{SFM}} = \boldsymbol{1} - \boldsymbol{T_{SFM}} - \boldsymbol{R_{SFM}} \tag{12}$$

$$\gamma = \frac{1-\sqrt{1-R_{corr}^2}}{1+\sqrt{1-R_{corr}^2}}\exp\left(-\frac{2L}{\lambda_{R,corr}}\right) \tag{13}$$

$$\lambda_{R,corr} = \frac{\lambda_0}{a\sqrt{1-R_{corr}^2}} \tag{14}$$

$$\lambda_0 = \frac{1}{NA_pQ_e} \tag{15}$$

$$a = 1 - Rp_f - \frac{4R^2p_s^2}{1-Rp_f-Rp_b-\ 2Rp_s} \tag{16}$$

$$b = Rp_b - \frac{4R^2 p_s^2}{1 - Rp_f - Rp_b - 2Rp_s} \quad (17)$$

$$R_{corr} = \frac{b}{a} \quad (18)$$

$$A_p Q_e = \sum (\pi\, d^2/4)\, pdf(d)\; w\; Q_e(d) \quad (19)$$

where T_{SFM}, R_{SFM}, A_{SFM}, is transmission, reflectance and absorbance calculated by TFM-2 or SFM, respectively. p_f, p_s and p_b are probability of forward, side and back scattering, λ_0 is characteristic extinction length, *pdf(d)* is the pdf calculated at droplet diameter *d*, $Q_e(d)$ is extinction efficiency calculated at droplet diameter *d* and *w* is the bin width. The rest of the parameters do not have physical meanings.

In this work, we aim to study transmission and absorption by aerosols theoretically in length scale relevant to aerosol photoreactors. We developed a novel way of calculating light transmission through scattering media with large size parameters which have significant forward scattering by shadow area model (SAM). The model is based on calculations of intersection areas of randomly distributed droplets. Then, we compare the model developed in this work to other theoretical models.

2. Methods

Intersection of randomly distributed droplets were computed by using Monte Carlo simulations in MATLAB R2020b. Model calculations of TFM and SAM were also computed in MATLAB R2020b.

COMSOL® Multiphysics 5.4 ray tracing model module is used to calculate the probability of forward and back scattering at several droplet diameters. A 2D model of one droplet was solved. Droplet diameter was changed from 50 to 300 µm. Length of the light source was the same as the droplet diameters. Therefore, all light rays coming out of the light source hit the droplet. Total number of light rays were 10000. Maximum amount of secondary light rays was set 500000. Extra fine mesh was applied to the droplets. A circle around the droplet was drawn (an accumulator) to count the light rays hitting the surfaces. Total amount of radiant flux that hit forward, side and back surfaces was calculated by integrating the total amount of radiant power ($W \cdot m^{-1}$) over these surfaces. Probability of forward and back scattering are calculated by dividing the radiant flux hitting one of these surfaces over the total radiant flux.

3. The shadow area model

As mentioned in the introduction, TFM and SFM can be used to solve for transmission and absorption. In this part, we present a novel approach to calculate the transmission and absorption in scattering media with large size parameters. Transmission and absorption can be calculated based on the shadow area of droplets. Grey scale of the shadow area can be considered as intersection area of many randomly distributed droplets. That is why, we call the model developed in this work as 'shadow area model' (SAM).

To the best of our knowledge, there is no distribution which is used to calculate the intersection areas of droplets. Poisson distribution is an ideal candidate since it expresses the probability of a given number of events occurring in a fixed interval of time and space if these events occur with a constant mean rate independently. Therefore, Poisson distribution can calculate probability of a light ray hitting one droplet or two droplets and so on. This is like ray tracing models. But, instead of using Monte Carlo simulations, an equation can be used. The cumulative distribution function of Poisson distribution is summation of a rate parameter, which is shown in Eq. (20). The rate parameter can be expressed as the cross sectional area of one droplet, aerosol number concentration and path length (Eq. (21)). Shadow areas casted by opaque droplets and transparent droplets are shown in Figure 2 **Error! Reference source not found.**a and b, respectively. The intersection areas of randomly distributed disks were calculated by Monte-Carlo simulations in MATLAB. These intersection areas are compared with each term of the summation in Poisson distribution in Figure 2 c. The intersection areas are predicted very well with Poisson distribution. Therefore, we could use this distribution to calculate transmission and absorption in a scattering media with a strong forward scattering.

$$F = e^{-\lambda} \sum_{n=0}^{\infty} \frac{\lambda^n}{n!} \tag{20}$$

where *F* is the cumulative distribution function and *λ* is the rate parameter.

$$\lambda = A_p N L Q_e \tag{21}$$

where A_p is projected (cross sectional) area of a droplet, *N* is aerosol number concentration, *L* is light path and Q_e is efficiency factor.

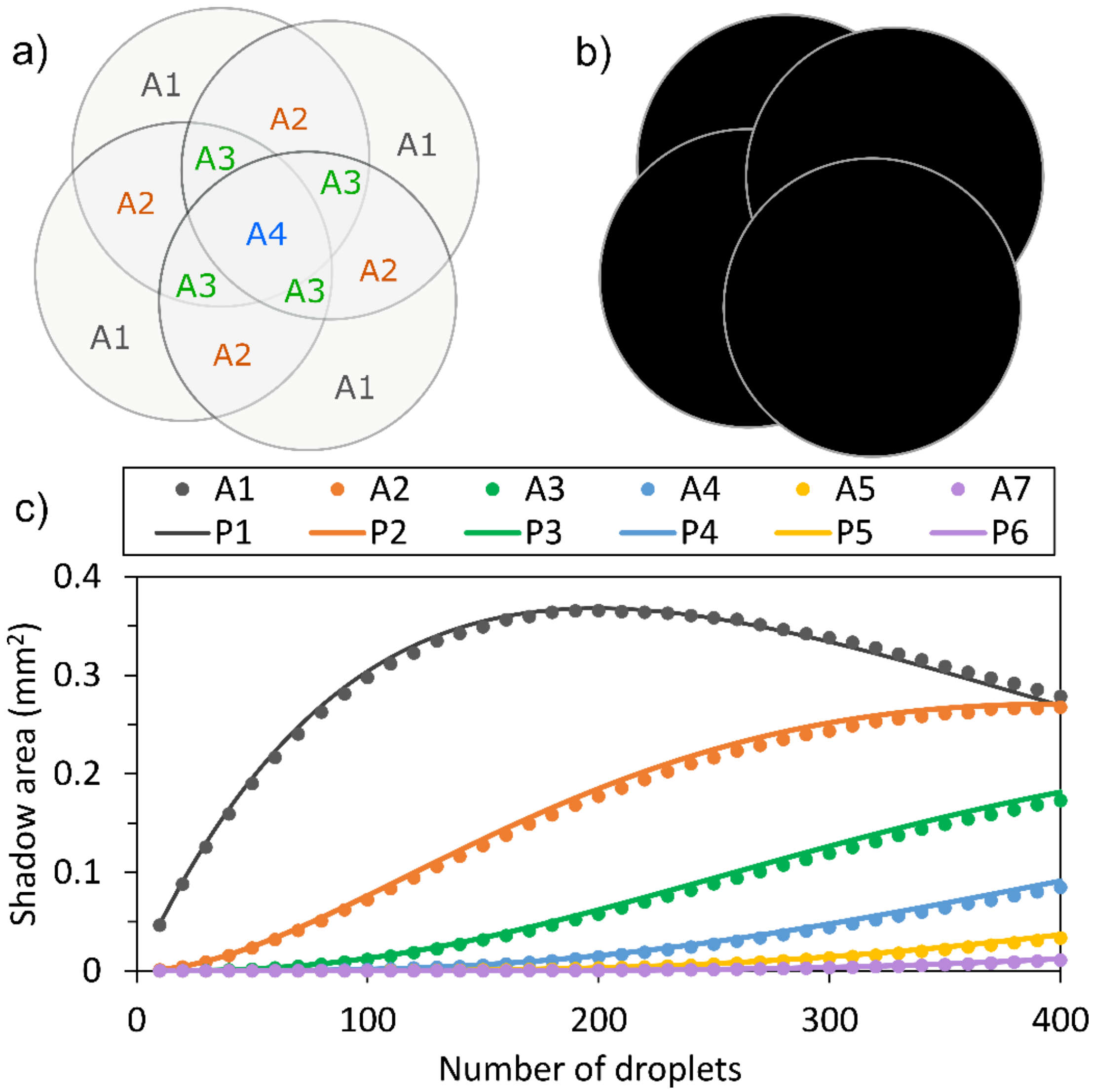

Figure 2. Shadow areas. a) Shadow area casted by opaque droplets. Beer's law corresponds to this image. b) Shadow areas casted by droplets transparent droplets in grey scale. TFM with both forward and back-scattering (TFM-2) and SFM might be represented with this image. c) Comparison of shadow areas calculated by Monte Carlo (A1 to A6) and by Poisson distribution (P1 to P6).

A photon balance can be performed on droplets considering that droplets are hypothetically casting a shadow area on each other as shown in Figure 3. Incoming radiant flux (G_0) is scattered around based on single-scattering albedo (R) which is shown previously in Eq. (4). Some of the scattered photons are scattered forward. This is expressed as multiplication of single-scattering albedo with transmittance (*t*). Photons that are scattered forward from the first droplet can hit another droplet and be scattered further away (which corresponds to area A2). Transmittance depends on phase function, which changed based on size parameter.

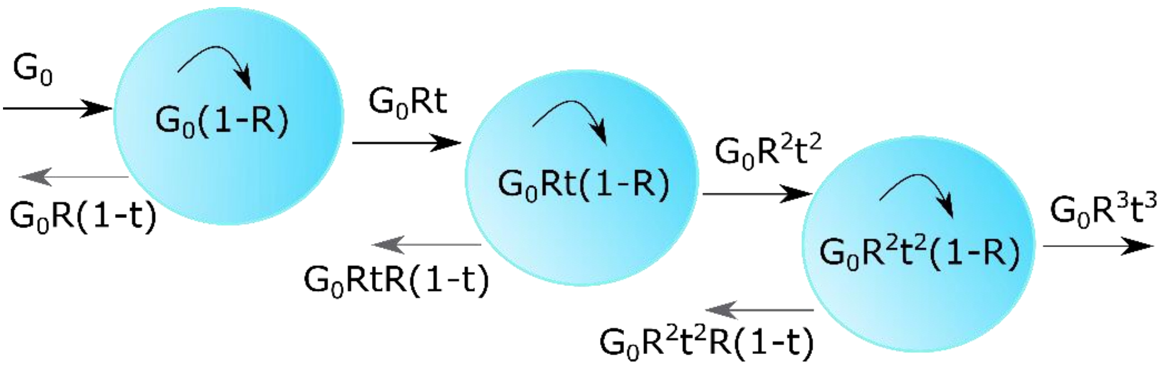

Figure 3. Photon balance on the droplets that are hypothetically casting a shadow area on each other.

The following assumptions are done while doing the photon balance:

1. All the photons that hit a droplet are absorbed.
2. Size parameter is large so geometric optics apply.
3. Back-scattered photons leave the system without interacting with other droplets.

These assumptions especially apply for optically thin systems with large size parameters where most of the incoming radiative flux is scattered forward. Based on the photon balance presented above, transmitted, absorbed and reflected radiant flux from the intersection area of n droplets can be expressed with Eqs (22), (23) and (24), respectively. The summation term that contains $R^n t^n$ can be simplified as shown in Eqn. (25).

$$G_{transmitted,n} = G_0 R^n t^n \tag{22}$$

$$G_{absorbed,n} = G_0 \sum_{n=0}^{n-1} R^n t^n (1 - R) \tag{23}$$

$$G_{reflected,n} = G_0 \sum_{n=0}^{n-1} R^n t^n R(1 - t) \tag{24}$$

$$\sum_{n=0}^{n-1} R^n t^n = \frac{1 - R^n t^n}{1 - Rt} \tag{25}$$

where $G_{transmitted,n}$, $G_{absorbed,n}$ *and* $G_{reflected,n}$ is radiant flux that is transmitted, absorbed and reflected from the *n*th droplet, respectively.

Total transmitted photons (or radiant flux) are summation of the photons that pass through the system without hitting any droplet and photons that are transmitted from droplets due to forward scattering. Photons that pass through the system without interacting with any droplet can be expressed as one minus the summation of the shadow area of all (opaque) droplets. Basically, this ends up in Beer's law. Photons that are transmitted through droplets can be found by summing up the photons that pass through the intersection areas, times the intersection areas (A_1, A_2, A_3 etc.). As a result, Eq. (22) is multiplied with the areas. The result is summed up when number of droplets (n) is going to infinity to obtain all photons that pass through.

$$G_{transmitted} = G_0 \left(1 - e^{-\lambda}\sum_{n=1}^{\infty}\frac{\lambda^n}{n!} + e^{-\lambda}\sum_{n=1}^{\infty}\frac{\lambda^n R^n t^n}{n!}\right) \tag{26}$$

$$T = \frac{G_{transmitted}}{G_0} = 1 - e^{-\lambda}\left(e^{\lambda} - 1\right) + e^{-\lambda}\left(e^{\lambda R t} - 1\right) \tag{27}$$

$$\boldsymbol{T_{SAM} = exp\,(-\lambda(1 - Rt))} \tag{28}$$

where $G_{transmitted}$ is total radiative flux that is transmitted and T is transmittance.

Absorption can be obtained by summing up all the absorbed photons when n is going to infinity (Eq. *(29)*). When Eq. (25) is implemented to Eq. (29), Eq. (30) is obtained which can be further simplified to Eq. (31).

$$G_{absorbed} = G_0\, e^{-\lambda}\sum_{n=1}^{\infty}\frac{\lambda^n}{n!}\left(\sum_{n=0}^{n-1} R^n t^n (1 - R)\right) \tag{29}$$

$$G_{absorbed} = G_0\,\frac{1 - R}{1 - Rt}\, e^{-\lambda}\sum_{n=1}^{\infty}\frac{\lambda^n}{n!}\,(1 - R^n t^n) \tag{30}$$

$$\boldsymbol{A_{SAM} = \frac{G_{absorbed}}{G_0} = \frac{1 - R}{1 - Rt}\left(1 - exp(-(1 - Rt)\lambda)\right)} \tag{31}$$

where $G_{absorbed}$ is the total radiative flux that is absorbed and A is absorbance.

In a similar manner, reflected (back-scattered) radiative flux can be obtained by summing up the photons coming out of all droplets (n goes to infinity) as shown in Eq. (32). By applying Eq. (25) to Eq. (32) and with further simplifications, Eq. (33) can be obtained.

$$G_{reflected} = G_0\, e^{-\lambda}\sum_{n=1}^{\infty}\frac{\lambda^n}{n!}\left(\sum_{n=0}^{n-1} R^n t^n R(1 - t)\right) \tag{32}$$

$$\boldsymbol{R_{SAM} = \frac{G_{absorbed}}{G_0} = \frac{R(1 - t)}{1 - Rt}\left(1 - exp\,(-(1 - Rt)\lambda)\right)} \tag{33}$$

where $G_{reflected}$ is reflected radiative flux and R_{SAM} is reflectance calculated by SAM.

Equations derived to calculate transmission, reflectance and absorption by SAM (Eq. (28), (31) and (33), respectively) are simpler compared to the ones found by SFM or TFM-2 which are shown in Eq. (10),(11) and (12). Equations found by SAM can be expressed by one line whereas to calculate transmission, reflectance of absorption by TFM-2 or SFM, the parameters in Eq. (12) to Eq. (18) need to be calculated. Therefore, SAM provides a better understanding of the relationship between the underlying parameters affecting transmission and absorption.

When R is going to zero, there is no scattering and all photons must be absorbed. Under this condition, droplets are casting an opaque shadow area. When R is going to zero, equation for T_{SAM} becomes the same as the one calculated by Beer's law (T_{BL}) whereas A_{SAM} goes to 1-T_{SAM} and R_{SAM} goes to zero. On the other extreme, when both R and t are going to one, all radiant flux is transmitted forward. Therefore, T_{SAM} is going to one whereas A_{SAM} and R_{SAM} are going to zero. In addition, the summation of A_{SAM}, T_{SAM} and R_{SAM} are one. Therefore, it can be concluded that the equations found here are consistent and represent the limits correctly.

In the work of Brucato et al [14], probabilities of forward, side and back scattering were fitted based on transmission calculations. Here, we report these probabilities at several water droplet diameters based on a COMSOL Multiphysics ray tracing model in

Table 1. For TFM-2, probabilities of forward and back scattering were calculated based on the radiant field that hits the hemispheres in the forward and back directions. Probabilities of forward and back scattering are around 0.95 and 0.05 for all droplet sizes. For SFM, radiant flux that goes up, down and to the sides are calculated by dividing the droplet (disk or circle in 2D) into 4 equal pieces. When the radiant field is divided into 4 equal sections, forward, side and back scattering values are around 0.90, 0.07 and 0.03. In the SFM model, p_s is divided by 4 since it is goes in 4 directions: up, down, right and left. These values are used to compute all the models. The transmittance (t) used in SAM is the same as forward scattering (p_f) used in other models.

Table 1. Probability of forward, side and back scattering used in the TFM-2 and SFM models. The values are obtained from a ray tracing model in COMSOL Multiphysics. Light is coming from the 180^o pointing towards 0^o.

Diameter (μm)	**TFM-2 model**		**SFM model**		
	Forward scattering (cos θ<0)	**Back scattering (cos θ<0)**	**Forward scattering (45^o<θ<315^o)**	**Side scattering (45^o<θ<135^o and 225^o <θ<315^o)**	**Back scattering (135^o<θ<225^o)**
50	0.980	0.020	0.917	0.066	0.017
100	0.961	0.039	0.903	0.067	0.030
150	0.965	0.035	0.912	0.063	0.025
200	0.951	0.048	0.902	0.065	0.032
250	0.951	0.049	0.904	0.065	0.031
300	0.949	0.050	0.906	0.062	0.031

Absorption and transmission calculated by SAM are compared with the ones calculated by Beer's law and TFM-1, TFM-2 and SFM in **Error! Reference source not found.**. Beer's law calculates both absorption and transmissions significantly different than other results. Therefore, it is not suitable for aerosol photoreactors. When R is low, more radiant power is absorbed and less radiant power is scattered. Therefore, as R decreases, transmission calculated by TFM-1 approaches to Beer's law since Beer's law assumes that all radiant flux is absorbed. TFM-1 is also not a good approximation for aerosol photoreactors as predicted since it does not account for forward scattering. SAM calculates both transmission and absorption with the same accuracy as TFM-2, which assumes both back and forward scattering. Results of both SAM and TFM-2 get closer to SFM when there is more absorption (low *R*). SFM is expected to give the most accurate results. However, the equations for SAM are much simpler and easier to understand compared to the ones for TFM and SFM while SAM still has a similar accuracy to these models. Therefore, SAM can provide an easier to implement and provides an easier grasp of the underlying physical phenomena.

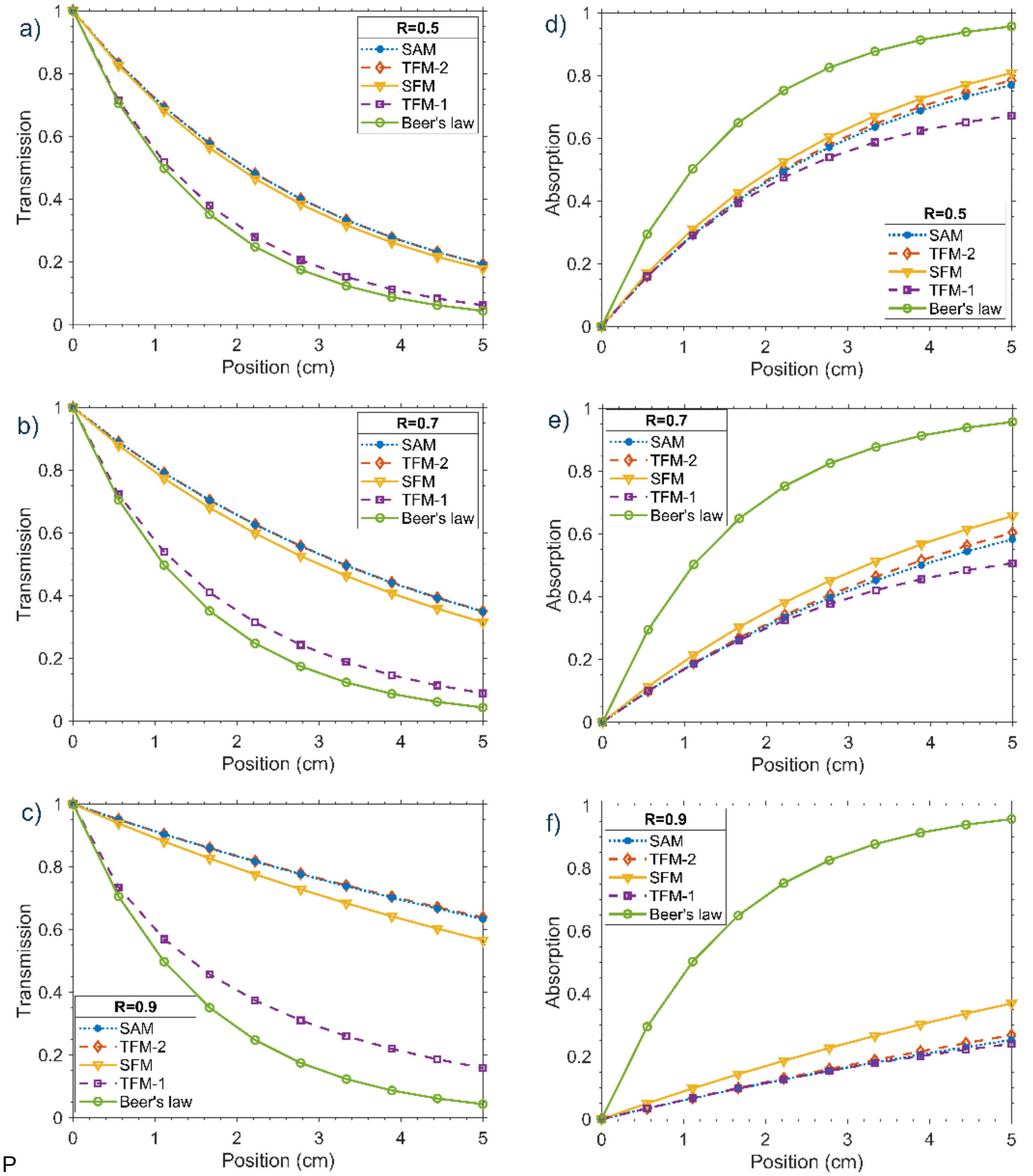

Figure 4. Comparison of different radiative transfer models in terms of transmission when a) *R*=0.50, b) *R*=0.70, c) *R*=0.90 and in terms of absorption when d) *R*=0.50, e) *R*=0.70, f) *R*=0.90. TFM-1 accounts for only back-scattering whereas TFM-2 and this work accounts for both forward and back scattering.

SFM accounts for scattering in 6 directions of the coordinate system. Droplet sizes were assumed to be 200 µm and aerosol number concentration was assumed to be 10^9 m^{-3}.

4. Conclusions

A novel way of calculating light transmission and absorption through scattering media is developed for aerosol photoreactor applications. We showed that Poisson distribution can be used to compute the intersection areas of randomly distributed disks. We used this distribution to calculate the intersection areas of droplets. By doing a photon balance, we were able to obtain a consistent set of equations for transmission, reflection and absorption. We call this model shadow area model (SAM). Probabilities of forward, side and back scattering were calculated by a COMSOL ray tracing model. They are used in the calculations of SAM, TFM-2 and SFM. SAM is compared with Beer's law, TFM-1, TFM-2 and SFM at varying single scattering albedos. Beer's law and TFM-1 are not appropriate for calculations of absorption and transmission in aerosol photoreactors. Their predictions were far from the predictions of TFM-2 and SFM. SAM was able to calculate transmission and absorption with the same accuracy as TFM-2 and with a similar accuracy to SFM. The equations derived for SAM here are simpler than the ones for TFM-2 and SFM. Yet, SAM is simpler compared to TFM-2 and SFM. Therefore, it provides an easier understanding of the physical phenomena.

5. Acknowledgments

M. E. Leblebici acknowledges Research Foundation Flanders (FWO) postdoctoral fellowship (39715) in Belgium for funding the research.

6. References

[1] E. Kayahan, M. Jacobs, L. Braeken, L.C.J. Thomassen, S. Kuhn, T. van Gerven, M.E. Leblebici, Dawn of a new era in industrial photochemistry: the scale-up of micro- and mesostructured photoreactors, Beilstein Journal of Organic Chemisty. 16 (2020) 2484–2504. https://doi.org/10.3762/bjoc.16.202.

[2] T. van Gerven, G. Mul, J. Moulijn, A. Stankiewicz, A review of intensification of photocatalytic processes, Chemical Engineering and Processing: Process Intensification. 46 (2007) 781–789. https://doi.org/10.1016/j.cep.2007.05.012.

[3] G.I. Ioannou, T. Montagnon, D. Kalaitzakis, S.A. Pergantis, G. Vassilikogiannakis, One-pot synthesis of diverse γ-lactam scaffolds facilitated by a nebulizer-based continuous flow photoreactor, ChemPhotoChem. 2 (2018) 860–864. https://doi.org/10.1002/cptc.201800068.

[4] G.I. Ioannou, T. Montagnon, D. Kalaitzakis, S.A. Pergantis, G. Vassilikogiannakis, A novel nebulizer-based continuous flow reactor: Introducing the use of pneumatically generated aerosols for highly productive photooxidations, ChemPhotoChem. 1 (2017) 173–177. https://doi.org/10.1002/cptc.201600054.

[5] G.I. Ioannou, T. Montagnon, D. Kalaitzakis, S.A. Pergantis, G. Vassilikogiannakis, Synthesis of cyclopent-2-enones from furans using a nebulizer-based continuous flow photoreactor, Organic and Biomolecular Chemistry. 15 (2017) 10151–10155. https://doi.org/10.1039/c7ob02557b.

[6] G.I. Ioannou, T. Montagnon, D. Kalaitzakis, S.A. Pergantis, G. Vassilikogiannakis, A novel nebulizer-based continuous flow reactor: Introducing the use of pneumatically generated aerosols for highly productive photooxidations, ChemPhotoChem. 1 (2017) 173–177. https://doi.org/10.1002/cptc.201600054.

[7] G.I. Ioannou, T. Montagnon, D. Kalaitzakis, S.A. Pergantis, G. Vassilikogiannakis, Synthesis of cyclopent-2-enones from furans using a nebulizer-based continuous flow photoreactor, Organic and Biomolecular Chemistry. 15 (2017) 10151–10155. https://doi.org/10.1039/c7ob02557b.

[8] G.I. Ioannou, T. Montagnon, D. Kalaitzakis, S.A. Pergantis, G. Vassilikogiannakis, One-pot synthesis of diverse γ-lactam scaffolds facilitated by a nebulizer-based continuous flow photoreactor, ChemPhotoChem. 2 (2018) 860–864. https://doi.org/10.1002/cptc.201800068.

[9] E. Kayahan, D. Urbani, P. Dambruoso, A. Massi, L. Braeken, T. van Gerven, M. Enis Leblebici, Overcoming mass and photon transfer limitations in a scalable reactor: Oxidation in an aerosol photoreactor, Chemical Engineering Journal. 408 (2021) 127357. https://doi.org/10.1016/j.cej.2020.127357.

[10] W.C. Hinds, Aerosol technology: properties, behavior, and measurements of airborne particles, 2nd ed., John Wiley & Sons, Inc, 1999.

[11] A. Brucato, L. Rizzuti, Simplified modeling of radiant fields in heterogeneous photoreactors. 1. Case of zero reflectance, Industrial and Engineering Chemistry Research. 36 (1997) 4740–4747. https://doi.org/10.1021/ie960259j.

[12] C. Mätzler, MATLAB functions for Mie scattering and absorption, 2002. https://omlc.org/software/mie/maetzlermie/Maetzler2002.pdf (accessed April 18, 2022).

[13] A. Brucato, L. Rizzuti, Simplified modeling of radiant fields in heterogeneous photoreactors. 2. Limiting “two-flux” model for the case of reflectance greater than zero, Industrial and Engineering Chemistry Research. 36 (1997) 4748–4755. https://doi.org/10.1021/ie960260i.

[14] A. Brucato, A.E. Cassano, F. Grisafi, G. Montante, L. Rizzuti, G. Vella, Estimating radiant fields in flat heterogeneous photoreactors by the six-flux model, AICHE Journal. 52 (2006) 3882–3890. https://doi.org/10.1002/aic.